Journal of the Optical Society of Korea, Vol. 9, No. 1, March 2005, pp. 6-12

Analysis of Fiber Nonlinearities by Perturbation Method

Jong-Hyung Lee* and Dae-Hyun Han

Department of Electronic Engineering, Dongeui University, Busan, 614-714, KOREA

Byeong-Yoon Choi

Department of Computer Engineering, Dongeui University, Busan, 614-714, KOREA

(Received October 22, 2003 : revised March 14, 2005)

The perturbation approach is applied to solve the nonlinear Schrödinger equation, and its valid range has been determined by comparing with the results of the split-step Fourier method over a wide range of parameter values. With $\gamma = 2km^{-1}mW^{-1}$, the critical distance for the first order perturbation approach is estimated to be $z_c \approx \frac{150}{P_{avg}}[km \cdot mW]$. The critical distance, z_c, is defined as the distance at which the normalized square deviation compared to the split-step Fourier method reaches 10^{-3}. Including the second order perturbation will increase z_c more than a factor of two, but the increased computation load makes the perturbation approach less attractive. In addition, it is shown mathematically that the perturbation approach is equivalent to the Volterra series approach, which can be used to design a nonlinear equalizer (or compensator). Finally, the perturbation approach is applied to obtain the sinusoidal response of the fiber, and its range of validity has been studied.

OCIS codes : 060.2430, 060.4370, 060.4510

I. INTRODUCTION

Recently, K. V. Peddanarappagari and M. Brandt-Pearce solved *the nonlinear Schrödinger equation* (NLSE) by the Volterra series transfer function approach [1,2,3]. Because this approach gives a closed-form solution, it can be a useful design tool for a nonlinear equalizer at the output of the fiber. Nonlinear impairments such as FWM (four-wave mixing) and XPM (cross-phase modulation) induced crosstalk are also evaluated using the Volterra series transfer function [4]. However, its complicated analytical form not only makes it hard to get physical insight, but also in many cases makes it less attractive in computational time compared to the split-step Fourier method. Additionally, its range of validity, that is, the valid range of the various physical parameters involved to assure accuracy within an allowable tolerance, has not been fully studied.

In this paper, the perturbation approach [5] is applied to solve the normalized NLSE, and it is shown mathematically that the approach is equivalent to the Volterra series transfer function method. Next, numerical results by the perturbation method will be compared with the result of the split-step Fourier method [6] to determine its valid range of parameters. Finally, the sinusoidal response of the normalized NLSE is solved by the perturbation method. In [7], it was demonstrated that the sinusoidal analysis could be an alternate, much simpler way of measuring eye opening penalty (EOP). Therefore, we may get a simple analytical expression to estimate EOP by the perturbation analysis.

II. PERTURBATION SOLUTION OF NORMALIZED NLSE

For pulse width $T_o \gtrsim 1$ps, the higher-order nonlinearities such as the stimulated Raman scattering (SRS) and the self-steepening have negligible effects, and the NLSE can be described in a simpler form by the normalized parameters as below [6]. The normalized NLSE will make it more convenient to treat various physical parameters in a unified way.

$$\frac{\partial U}{\partial \xi} = -\frac{1}{2} i \cdot \mathrm{sgn}(\beta_2) \frac{\partial^2 U}{\partial \tau^2} + iN^2 |U|^2 U \tag{1}$$

where β_2[ps^2/km] is the second order propagation con-

stant, $N^2 = \frac{L_D}{L_N} = \frac{\gamma P_{avg} T_o^2}{|\beta_2|}$ $\left(L_D = \frac{T_o^2}{|\beta_2|}, L_N = \frac{1}{\gamma P_{avg}} \right)$, γ = fiber nonlinearity $\tau = t/T_o$, $\xi = z/L_D$, and $U(\xi, \tau)$ is the slowly varying envelope normalized by the path averaged power, P_{avg}.

In general, the solution of the NLSE can not be found in analytical form except for solitons. Therefore, typical optical communication systems usually require numerical approaches to solve the NLSE. While a numerical approach like the split-step Fourier method is known to be accurate, it is time consuming and doesn't provide any physical insight. In this work, we will attempt to find the perturbation solution of the normalized NLSE. While the perturbation approach may not give a solution as accurate as numerical approaches, the approach can provide better physical insight to understand how dispersion and nonlinearity interact. To find the perturbation solution of the normalized NLSE, let

$$U(\xi,\tau) = U^{(0)}(\xi,\tau) + \varepsilon V^{(1)}(\xi,\tau) + \varepsilon^2 V^{(2)}(\xi,\tau) + \cdots \quad (2)$$

where $\varepsilon = N^2$, $U^{(0)}(\xi,\tau)$ is the solution of the dispersion alone case, and $\varepsilon V^{(1)}(\xi,\tau)$ is the first-order nonlinear solution, $\varepsilon^2 V^{(2)}(\xi,\tau)$ is the second-order solution, and so forth.

In the dispersion alone case, Eq. (1) degenerates into the linear partial differential equation and the solution has the form

$$u(\xi,\omega) = u(0,\omega)\exp\left[\frac{i}{2}\mathrm{sgn}(\beta_2)\omega^2\xi\right] \quad (3)$$

where $u = \Im[U(\xi,\tau)]$. $\Im\{\bullet\}$ denotes Fourier transform with respect to τ, and $u(0,\omega)$ is the Fourier transform of the incident field at $\xi = 0, U(0,\tau)$.

By putting Eq. (2) into Eq. (1), and by equating the terms proportional to ε^n separately for each value of n, we will get consecutive equations as below.

$$i\frac{\partial U^{(0)}}{\partial \xi} = \mathrm{sgn}(\beta_2)\frac{1}{2}\frac{\partial^2 U^{(0)}}{\partial \tau^2} \quad (4)$$

$$i\frac{\partial V^{(1)}}{\partial \xi} = \mathrm{sgn}(\beta_2)\frac{1}{2}\frac{\partial^2 V^{(1)}}{\partial \tau^2} - \left|U^{(0)}\right|^2 U^{(0)} \quad (5)$$

$$i\frac{\partial V^{(2)}}{\partial \xi} = \mathrm{sgn}(\beta_2)\frac{1}{2}\frac{\partial^2 V^{(2)}}{\partial \tau^2} - \left\{2\left|U^{(0)}\right|^2 V^{(1)} + U^{(0)}(V^{(1)})^* U^{(0)}\right\} \quad (6)$$

$$\vdots$$

Here, * denotes the complex conjugate.

Eq. (2) can also be expressed in the frequency domain as follows.

$$u(\xi,\omega) \approx u^{(0)}(\xi,\omega) + u^{(1)}(\xi,\omega) + u^{(2)}(\xi,\omega) + \Lambda \quad (7)$$

where $u^{(0)}(\xi,\omega)$ is the solution of the dispersion alone case which is given by Eq. (3). Higher order terms in the frequency domain are defined to include N parameter for simplicity such that $u^{(1)}(\xi,\omega) = \Im\left[\varepsilon V^{(1)}(\xi,\tau)\right]$, $u^{(2)}(\xi,\omega) = \Im\left[\varepsilon^2 V^{(2)}(\xi,\tau)\right]$, and so on. In the frequency domain, higher order terms are solutions of coupled ordinary differential equations. From Eqs. (5) and (6),

$$\frac{\partial u^{(1)}(\omega,\xi)}{\partial \xi} = \frac{j}{2}\mathrm{sgn}(\beta_2)\omega^2 u^{(1)}(\omega,\xi) + jN^2\Im\left\{\left|U^{(0)}(\tau,\xi)\right|^2 U^{(0)}(\tau,\xi)\right\} \quad (8)$$

$$\frac{\partial u^{(2)}(\omega,\xi)}{\partial \xi} = \frac{j}{2}\mathrm{sgn}(\beta_2)\omega^2 u^{(2)}(\omega,\xi) + jN^2\Im\left\{2\left|U^{(0)}(\tau,\xi)\right|^2 U^{(1)}(\tau,\xi) + U^{(0)}(\tau,\xi)\left(U^{(1)}(\tau,\xi)\right)^* U^{(0)}(\tau,\xi)\right\} \quad (9)$$

$$\vdots$$

where $U^{(1)}(\tau,\xi) = \varepsilon V^{(1)}(\xi,\tau)$.

By solving Eqs (4), (5), (or Eqs (8), (9)) and so forth in a consecutive way, we can obtain an approximate solution of the NLSE. We may expect that including higher order terms will improve the accuracy of the perturbed solution of Eq. (7). However, calculations of higher order terms will increase the numerical load tremendously, which makes the perturbation approach less attractive. Therefore it will be interesting to find the valid range of N and propagation distance for which the perturbation solution, up to the first or the second order terms, is valid within a given tolerance. The valid range of parameter values will be discussed in the next section.

III. COMPARISON OF PERTURBATION SOLUTION WITH SPLIT-STEP FOURIER METHOD

In this section, the valid range of the perturbation solution developed in the previous section will be determined. The split-step Fourier method will be used as a reference, and its accuracy will be addressed first by comparing with known theoretical predictions. It is known that Eq. (1) leads to soliton solutions by applying the inverse scattering method [6]. That is, when the input pulse is $U(0,\tau) = \mathrm{sech}(\tau)$, the analytical solution to Eq.(1) in the anomalous dispersion region

with N=1 gives [6]

$$U(\xi,\tau)=sech(\tau)\exp(-j\xi/2) \tag{10}$$

Eq. (10) is ideally suited to see the accuracy of the split-step Fourier method because the solution is the result of interplay between dispersion and nonlinearity, and it has a simple form. Figure 1 compares Eq. (10) with the simulation result by the split-step Fourier method at ξ=z/LD=15. From the figure, we can observe that the difference between the two curves is negligible. (Note the magnitude scale is logarithmic.) Since typical values of LD are in the range of a few hundred km to thousand km, the simulation distance ξ=15 could be over transoceanic distances. In the simulation, the step size $\Delta\xi = 0.01$ is used, which will result in 0.01 rad of the maximum phase shift by the nonlinear operator

To compare two curves generated by two different methods, say, 'A' method and 'B' method, *the normalized square deviation* (NSD) is defined as [1],

$$NSD(\xi)=\frac{\int_{-\infty}^{\infty}|U_A(\xi,\tau)-U_B(\xi,\tau)|^2 d\tau}{\int_{-\infty}^{\infty}|U(0,\tau)|^2 d\tau} \tag{11}$$

where $U_A(\xi,\tau)$ = output field envelope by method 'A', and $U_B(\xi,\tau)$ = output field envelope by method 'B'. Figure 2 shows the calculated NSDs as a function of propagation distance resulting from the split-step method compared to the analytical solution, Eq.(10). We

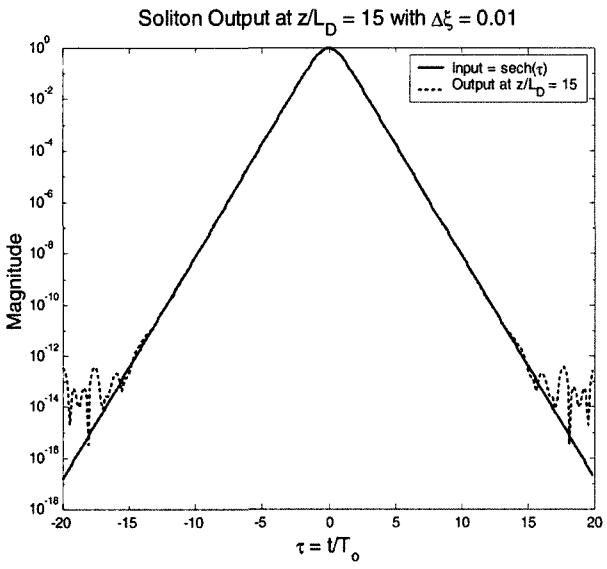

FIG. 1. Comparison of fundamental soliton output by the split-step Fourier method with theoretical prediction.

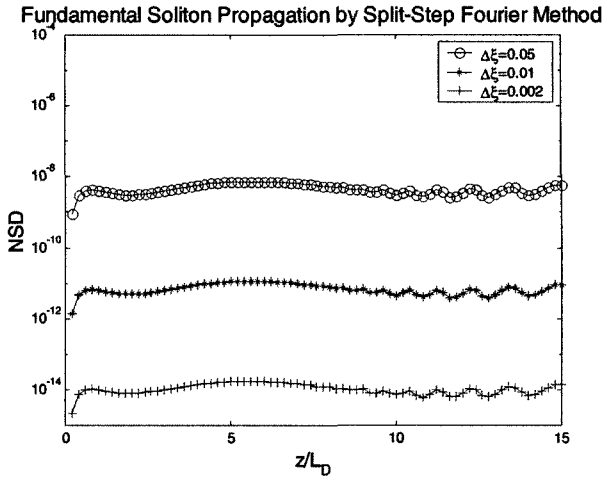

FIG. 2. NSD evolutions of soliton transmission by the split-step Fourier method.

observe that the NSD is greatly affected by the simulation step size $\Delta\xi$ as expected. However, NSDs remain almost constant at very small values up to the transmission distance ξ=15. For example, when $\Delta\xi = 0.01$, the NSD remains below 10^{-11} up to ξ=15. These results indicate that the split-step Fourier method is very reliable, and can serve as a reference to measure the valid range of perturbation method if $\Delta\xi$ is small enough. For the remainder of this work, $\Delta\xi = 0.01$ will be used for the split-step method.

Now the perturbation solution of the normalized NLSE is compared with simulation results. Input pulse

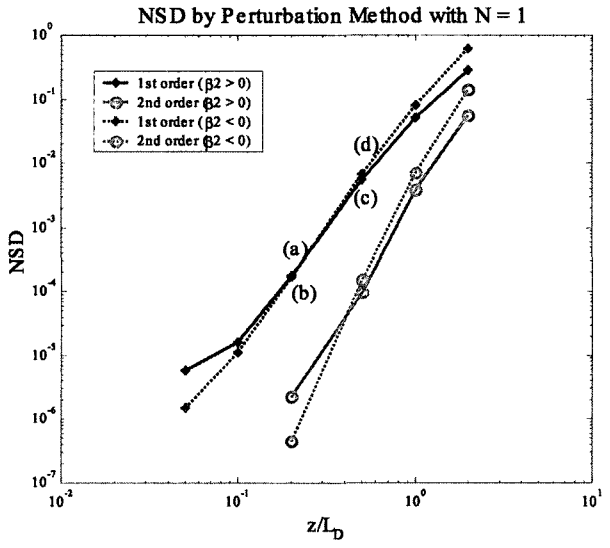

FIG. 3. NSD by perturbation method with N=1 (solid with* = 1st order and $\beta_2 > 0$, dash dot with* = 1st order and $\beta_2 < 0$, solid with o = 2nd order and $\beta_2 > 0$, dash dot with o = 2nd order and $\beta_2 < 0$).

shape is assumed to be a Gaussian such that $U(0,\tau) = \exp\left(-\frac{1}{2}\tau^2\right)$. Figure 3 shows the NSD between perturbation solutions and numerical simulations when N =1. As expected, the perturbation solutions up to the second order give about one order smaller NSD's compared to the results from the first order solutions. However, as the propagation distance increases, the perturbation solution results in larger errors (larger NSD values) regardless of dispersion region. These results suggest that the perturbation solution is limited in its numerical accuracy compared to the split-step method. Figure 4 compares output pulse shapes by the first order perturbation solution with split-step simulation results at ξ=0.2 ((a) and (b)) and at ξ=0.5 ((c) and (d)). When ξ=0.5, the differences between the two curves become noticeable while the differences are negligible when ξ=0.2 To decide the valid range of parameters for use of the perturbation solution, we need to determine an allowable tolerance level. From Figure 3 and Figure 4, the maximum allowable NSD value is chosen to be 10^{-3}, which occurs between (a) and (c) in Figure 3.

Figure 5 shows the critical distance (= ξ_C), which is defined as the distance at which NSD =10^{-3}, as a function of N. The curves of ξ_C in logarithmic plots are almost straight lines for a broad range of N values. The good linearity between the calculated ξ_C and N^2 indicates a near constant value for their product. That is,

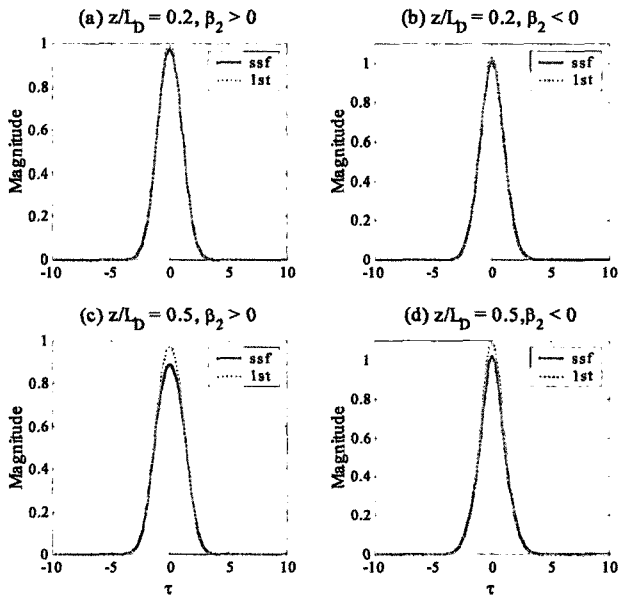

FIG. 4. Comparison of pulse shapes by the first order perturbation method and split-step method (a) z/L_D =0.2, β_2 >0, (b) z/L_D =0.2, β_2 <0, (c) z/L_D =0.5, β_2 >0, (d) z/L_D =0.5, β_2 <0.

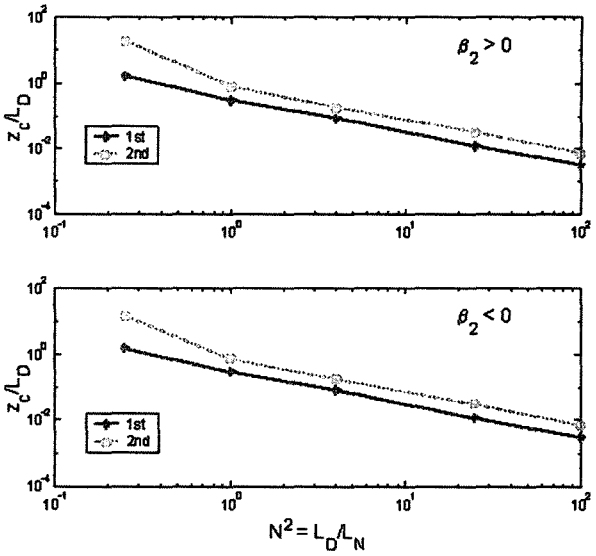

FIG. 5. Normalized critical distances at NSD = 10^{-3} (a) $\beta_2 > 0$ (*: 1st order, o: 2nd order) (b) $\beta_2 < 0$ (*: 1st order, o: 2nd order).

the first order perturbation solution gives $N^2\xi_c = N^2\frac{z_c}{L_D} = \frac{z_c}{L_N} \approx 0.3$ in both the normal and anomalous dispersion regions. When the second order is included, the product is approximately 0.7. Since $N^2 = L_D/L_N$, and $L_N = 1/\gamma P_{avg}$, we can estimate the critical distance z_c. With $\gamma = 2km^{-1}mW^{-1}$, the critical distance by the first order perturbation is estimated as $z_c \approx \frac{150}{P_{avg}}[km\cdot mW]$. For example, if we take the peak power P_o=2mW, and amplifier spacing is assumed to be 80km with 0.25dB/km loss of the fiber, the path-averaged power is P_{avg} = 0.43mW ($P_{avg} = \frac{1}{z_a}\int_0^{z_a} P_o e^{-\alpha z} dz = \frac{P_o}{\alpha z_a}(1-e^{-\alpha z_a})$), this results in $z_c \approx$350km. This means that we can get less than 10^{-3} of NSD using the first order perturbation solution up to z = 350km. When we include the second order term, the critical distance extends to nearly 800km. However, Figure 3 indicates that the critical distances can be substantially shorter if a smaller value of NSD is required to have more accurate results.

IV. SINUSOKDAL RESPONSE USING PERTURBATION ANALYSIS

In reference [7], it was demonstrated that the sinusoidal analysis could be an alternate much simpler way of measuring eye-opening penalty (EOP). In this section, the sinusoidal response of the NLSE is solved by the perturbation method developed in section 2.

From Eq. (5), the first-order perturbed output, $U^{(1)}(\xi, \tau)$

$=\varepsilon V^{(1)}(\xi,\tau)$, is related to the linear output, $U^{(0)}(\zeta,\tau)$, as below.

$$\frac{\partial U^{(1)}(\zeta,\tau)}{\partial\xi}=-\frac{j}{2}\frac{\partial^2 U^{(1)}(\xi,\tau)}{\partial\tau^2}+jN^2\left|U^{(0)}(\xi,\tau)\right|^2U^{(0)}(\xi,\tau) \quad (12)$$

In Eq.(12), the fiber is assumed to be in the normal dispersion region where the sinusoidal analysis has a broader range of agreement with EOP than in the anomalous region. When the input sinusoid is given as the raised-cosine form $(U(0,\tau)=\frac{1}{2}+\frac{1}{2}\cos\omega_p\tau)$, $U^{(0)}(\xi,\tau)=\frac{1}{2}+\frac{1}{2}e^{\frac{j}{2}\omega_p^2\xi}\cos\omega_p\tau$ from Eq. (4), which will make the nonlinear term in Eq. (12) periodic. Therefore the first-order perturbed output $U^{(1)}(\zeta,\tau)$ will also be periodic, and we can express the first-order output in terms of a Fourier series.

$$U^{(1)}(\xi,\tau)=\sum_{n=-\infty}^{\infty}C_n^{(1)}(\xi)e^{jn\omega_p\tau} \quad (13)$$

with initial condition $C_n^{(1)}(0)$ = 0 for all n.

The Fourier series coefficients, Cn(1), can be evaluated by putting Eq. (13) into Eq. (12) and then equating terms of the same frequency. Since the highest frequency component in $\left|U^{(0)}(\xi,\tau)\right|^2U^{(0)}(\xi,\tau)$is 3ωp, we need to set up differential equations up to n = 3. The resulting Fourier series coefficients for each n value up to n = 3 are

$$\text{n}=0,\ C_0^{(1)}(\xi)=\frac{N^2}{16\omega_p^2}\left(\cos\omega_p^2\xi-1\right)+j\left(\frac{1}{4}N^2\xi+\frac{N^2}{16\omega_p^2}\sin\omega_p^2\xi\right)$$

$$\text{n}=1,\ C_1^{(1)}(\xi)=\frac{N^2}{32\omega_p^2}\left(\cos\left(\frac{3}{2}\omega_p^2\xi\right)-\cos\left(\frac{\omega_p^2\xi}{2}\right)\right)$$
$$\left.-\frac{11}{64}N^2\xi\sin\left(\frac{\omega_p^2\xi}{2}\right)+jN^2\left(\frac{1}{8\omega_p^2}\sin\left(\frac{\omega_p^2\xi}{2}\right)+\frac{11}{64}\xi\cos\left(\frac{\omega_p^2\xi}{2}\right)\right)\right|$$

$$\text{n}=2,\ C_2^{(1)}(\xi)=\frac{N^2}{32\omega_p^2}\left[2\cos(2\omega_p^2\xi)-\cos(\omega_p^2\xi)\right.$$
$$\left.-1+j\left(2\sin(2\omega_p^2\xi)-\sin(\omega_p^2\xi)\right)\right]$$

$$\text{n}=3,\ C_3^{(1)}(\xi)=\frac{N^2}{256\omega_p^2}\left[\cos(\frac{9}{2}\omega_p^2\xi)-\cos(\omega_p^2\xi)\right.$$
$$\left.-1+j\left(\sin(\frac{9}{2}\omega_p^2\xi)-\sin(\omega_p^2\xi)\right)\right]$$

Now the output field is approximated as the sum of the linear solution and the first-order perturbation solution such that

$$\begin{aligned}U(\xi,\tau)&\approx U^{(0)}(\xi,\tau)+U^{(1)}(\xi,\tau)\\&=\left[C_o^{(0)}+C_1^{(0)}f(\omega_p)\right]+\left[C_o^{(1)}+C_1^{(1)}f(\omega_p)+C_2^{(1)}f(2\omega_p)+C_3^{(1)}f(3\omega_p)\right]\\&=\left(C_o^{(0)}+C_o^{(1)}\right)+\left(C_1^{(0)}+C_1^{(1)}\right)f(\omega_p)+C_2^{(1)}f(2\omega_p)+C_3^{(1)}f(3\omega_p)\\&=C_o+C_1f(\omega_p)+C_2f(2\omega_p)+C_3f(3\omega_p)\end{aligned} \quad (14)$$

where $f(\omega_p)=e^{j\omega_p\tau}+e^{-j\omega_p\tau}$, $\frac{\omega_p}{2\pi}=\frac{1}{2}$, and

$$C_o=C_o^{(0)}+C_o^{(1)}=\left[\frac{1}{2}-\frac{N^2}{16\omega_p^2}\left(1-\cos\omega_p^2\xi\right)\right]-j\left[\frac{1}{4}N^2\xi+\frac{N^2}{16\omega_p^2}\sin\omega_p^2\xi\right]$$

$$\begin{aligned}C_1&=C_1^{(0)}+C_1^{(1)}\\&=\left(\frac{1}{4}-\frac{N^2}{32\omega_p^2}\right)\cos\left(\frac{\omega_p^2\xi}{2}\right)+\frac{N^2}{32\omega_p^2}\cos\left(\frac{3}{2}\omega_p^2\xi\right)-\frac{11}{64}N^2\xi\sin\left(\frac{\omega_p^2\xi}{2}\right)\\&\quad+jN^2\left(\left(\frac{1}{4}+\frac{1}{8\omega_p^2}\right)\sin\left(\frac{\omega_p^2\xi}{2}\right)+\frac{11}{64}\xi\cos\left(\frac{\omega_p^2\xi}{2}\right)\right)\end{aligned}$$

$$C_2=C_2^{(1)}$$

$$C_3=C_3^{(1)}$$

Finally, the output optical power signal is obtained as

$$\begin{aligned}P(\xi,\tau)&=\left|U(\xi,\tau)\right|^2\approx\left|U^{(0)}(\xi,\tau)+U^{(1)}(\xi,\tau)\right|^2\\&=\left|C_o+C_1f(\omega_p)+C_2f(2\omega_p)+C_3f(3\omega_p)\right|^2\end{aligned} \quad (15)$$

Eq. (15) has various frequency components. However, we are interested only in the ωp component (the fundamental Fourier series component), which is expressed as

$$P(\xi,\tau)\big|_{\omega_p}=2\left\{\text{Re}\left(C_oC_1^*\right)+\text{Re}\left(C_1C_2^*\right)+\text{Re}\left(C_2C_3^*\right)\right\} \quad (16)$$

where* denotes the complex conjugate.

It is worth remembering that the perturbation analysis has a limited range of applicability because of accuracy as discussed in section 3. To estimate the valid range of Eq. (16), the critical distance at NSD = 10-3 using the first-order perturbation solution is plotted in Figure 6 (a). The NSD curve compares the distance of 1dB SRP (sinusoidal response penalty) resulting from simulations as a function of N2. SRP is defined as

$$SRP[dB]=-10\log\left(\frac{|C_1(\xi)|}{|C_1(0)|}\right) \quad (17)$$

where $\left|C_1(\xi)\right|$ is the magnitude of the fundamental Fourier series coefficient of the received signal at ξ. Figure 6 (a) indicates that Eq.(16) can be used when N^2 is less than 3. In Figure 6 (b), the $\left|C_1(\xi)\right|$ by simulation is compared with Eq. (16) when N^2 = 3. The

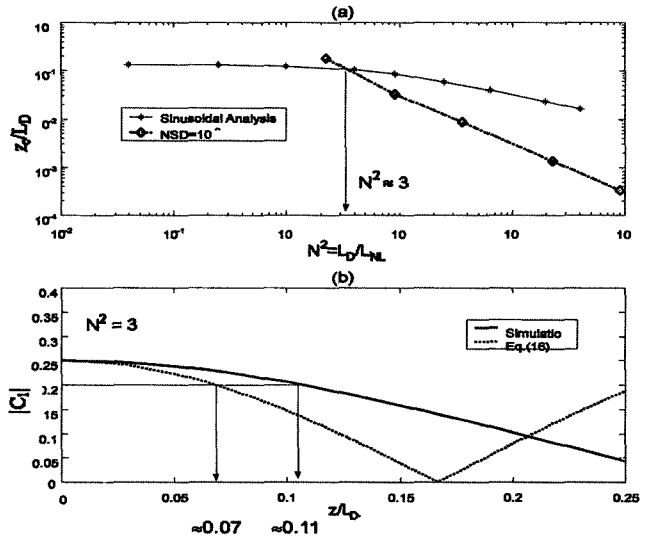

FIG. 6. (a) Comparison of the critical distance at NSD = 10^{-3} using up to the first order perturbation solution and the simulated 1dB penalty distance of sinusoidal response in the normal dispersion region. (b) Comparison of the fundamental Fourier series coefficient, $|C_1|$ when $N^2 = 3$.

normalized distance corresponding to 1 dB SRP is around 0.07 from Eq. (16), but the simulation result gives approximately 0.11. For better accuracy, we may include higher-order perturbed solutions in Eq. (16). However, for a modest fiber nonlinearities ($N^2 < 3$), the perturbation approach can be used to get a first order system degradation due to fiber dispersion and fiber nonlinearities.

V. CONCLUSIONS

We have shown that the perturbation approach is equivalent to the Volterra series method at least up to the third-order of the Volterra approach which is appealing for design of a nonlinear compensator due to its closed form solution. In this paper, we determined the validity range of the perturbation approach (that is, the Volterra approach) and the sinusoidal response of the NLSE is also solved by the perturbation method to have an analytical, thus much simpler means of system evaluation.

We found that the critical distance at which NSD reaches its maximum allowable value (10^{-3}, in this work) is inversely proportional to the average pulse power, P_{avg}. The proportionality is evaluated to be around 150 [km · mW]. The second-order solution will increase the critical distance more than a factor of two, but the increased computation load makes it less attractive. This is mainly because the motivation of the perturbation approach (or Volterra approach) is not for computational efficiency but for a possible analytical tool to optimize a nonlinear fiber link with a nonlinear equalizer. Finally, the sinusoidal response has also been derived analytically based on the perturbation analysis. Since the perturbation analysis has a limited range of validity, the derived analytical expression also has a limited range of applicability. Comparison with numerical results reveals that the derived expression may be used when $N^2 < 3$. Within this range, the analytically expressed sinusoidal response can be used to optimize a nonlinear fiber link to a first order.

ACKNOWLEDGMENT

The present research was conducted by the research fund of Dongeui University in 2004.

*Corresponding author : jonghlee@deu.ac.kr

APPENDIX

Perturbation Approach and Volterra Series Transfer Function

In the Volterra series approach [1], the linear transfer function, $H_1(\xi,\omega)$, and the third-order nonlinear transfer function (third-order Volterra kernel), $H_3(\xi, \omega_1, \omega_2, \omega_3)$, can be expressed as below in the normalized units ($H_2(\xi, \omega_1, \omega_2,) = 0$),

$$H_1(\xi,\omega) = \exp\left[\frac{i}{2}\mathrm{sgn}(\beta_2)\omega^2\xi\right] \tag{A.1}$$

$$H_3(\omega_1,\omega_2,\omega_3,\xi) = jN^2 \frac{\exp\left[\frac{j}{2}\mathrm{sgn}(\beta_2)(\omega_1^2-\omega_2^2+\omega_3^2)\xi\right]-\exp\left[\frac{j}{2}\mathrm{sgn}(\beta_2)(\omega_1-\omega_2+\omega_3)^2\xi\right]}{\frac{j}{2}\mathrm{sgn}(\beta_2)(\omega_1^2-\omega_2^2+\omega_3^2)-\frac{j}{2}\mathrm{sgn}(\beta_2)(\omega_1-\omega_2+\omega_3)^2} \tag{A.2}$$

Therefore, the normalized field spectrum is approximated as below by ignoring higher order terms.

$$\begin{aligned} u(\omega,\xi) &\approx u_V^{(1)}(\omega,\xi)+u_V^{(3)}(\omega,\xi) \\ &= H_1(\omega,\xi)u(\omega)+\frac{1}{(2\pi)^2}\iint H_3(\omega_1,\omega_2,\omega-\omega_1 \\ &\quad +\omega_2,\xi)u(\omega_1)u^*(\omega_2)u(\omega-\omega_1+\omega_2)d\omega_1 d\omega_2 \end{aligned} \tag{A.3}$$

where $u(\omega)=u(\omega,0)$.

In Eq.(A.3), $u_V^{(1)}(\omega,\xi)$ is equivalent to the unperturbed solution, $u^{(0)}(\omega,\xi)$, because both are the linear solution of the NLSE. In addition, we can show that the third-order Volterra kernel output, $u_V^{(3)}(\omega,\xi)$, is equivalent to the first-order perturbed solution, $u^{(1)}(\omega,\xi)$ in Eq. (7).

By differentiating $u_V^{(3)}(\omega,\xi)$ with respect to ξ,

$$\frac{\partial u_V^{(3)}(\omega,\xi)}{\partial \xi} = \frac{1}{(2\pi)^2}\iint \frac{\partial H_3(\omega_1,\omega_2,\omega-\omega_1+\omega_2,\xi)}{\partial \xi} u(\omega_1)u^*(\omega_2)u(\omega-\omega_1+\omega_2)d\omega_1 d\omega_2 \tag{A.4}$$

where

$$\frac{\partial H_3(\omega_1,\omega_2,\omega-\omega_1+\omega_2,\xi)}{\partial \xi} = j\frac{1}{2}\mathrm{sgn}(\beta_2)(\omega_1-\omega_2+\omega_3)^2 H_3(\omega_1,\omega_2,\omega_3,\xi) + jN^2 H_1(\omega_1,\xi)H_1^*(\omega_2,\xi)H_1(\omega_3,\xi)$$

Then

$$\begin{aligned}\frac{\partial u_V^{(3)}(\omega,\xi)}{\partial \xi} &= \frac{1}{(2\pi)^2}\iint j\frac{1}{2}\mathrm{sgn}(\beta_2)\omega^2 H_3(\omega_1,\omega_2,\omega-\omega_1 \\ &\quad +\omega_2,\xi)u(\omega_1)u^*(\omega_2)u(\omega-\omega_1+\omega_2)d\omega_1 d\omega_2 \\ &\quad +\frac{1}{(2\pi)^2}\iint jN^2 H_1(\omega_1,\xi)H_1^*(\omega_2,\xi)H_1(\omega-\omega_1 \\ &\quad +\omega_2,\xi)u(\omega_1)u^*(\omega_2)u(\omega-\omega_1+\omega_2)d\omega_1 d\omega_2 \\ &= \frac{j}{2}\omega^2\,\mathrm{sgn}(\beta_2)u_V^{(3)}(\omega,\xi)+\frac{jN^2}{(2\pi)^2}\iint H_1(\omega_1,\xi)H_1^*(\omega_2,\xi)H_1(\omega \\ &\quad -\omega_1+\omega_2,\xi)u(\omega_1)u^*(\omega_2)u(\omega-\omega_1+\omega_2)d\omega_1 d\omega_2 \\ &= \frac{j}{2}\omega^2\,\mathrm{sgn}(\beta_2)u_V^{(3)}(\omega,\xi) \\ &\quad + jN^2\left\{\frac{1}{(2\pi)^2}\iint u_V^{(1)}(\omega_1,\xi)\left[u_V^{(1)}(\omega_2,\xi)\right]^* u_V^{(1)}(\omega-\omega_1+\omega_2,\xi)d\omega_1 d\omega_2\right\} \\ &= \frac{j}{2}\mathrm{sgn}(\beta_2)\omega^2 u_V^{(3)}(\omega,\xi)+jN^2\Im\left\{U^{(0)}(\tau,\xi)\left|U^{(0)}(\tau,\xi)\right|^2\right\}\end{aligned} \tag{A.5}$$

where $u_V^{(1)}(\omega,\xi)=\Im\{U^{(0)}(\tau,\xi)\}$

The resulting equation has the same form of Eq. (8) which comes from the perturbation approach. Therefore we can conclude that both of these approaches are equivalent at least up to the third-order of the Volterra approach.

REFERENCES

[1] K. V. Peddanarappagari and M. Brandt-Pearce, "Volterra series transfer function of single-mode fibers," *Journal of Lightwave Technology*, vol. 15, no. 12, pp. 2232- 2241, Dec. 1997.

[2] K. V. Peddanarappagari and M. Brandt-Pearce, "Volterra series approach for optimizing fiber-optic communications system designs," *Journal of Lightwave Technology*, vol. 16, no. 11, pp. 2046-2055, Nov. 1998.

[3] B. Xu and M. Brandt-Pearce, "Modified Volterra series transfer function method," *IEEE Photonics Technology Letters*, vol. 14, no. 1, pp. 47-49, Jan. 2002.

[4] B. Xu and M. Brandt-Pearce, "Comparison of FWM- and XPM-induced crosstalk using the Volterra series transfer function method," *Journal of Lightwave Technology*, vol. 21, no. 1, pp. 40-53, Jan. 2003.

[5] A. H. Nayfeh, *Introduction to Perturbation Techniques*, John Wiley & Sons, Inc. 1981.

[6] G. P. Agrawal, *Nonlinear Fiber Optics*, Second Ed., Academic Press, San Diego, 1995.

[7] Jong-Hyung Lee, Dae-Hyun Han, and Byeong-Yoon Choi, "Analysis of system performance degradation using sinusoidally modulated signal in optical fiber communication systems," *Journal of Optical Society of Korea*, vol. 8, no. 2, pp. 59-64, June 2004.